Dissociable Network Properties of Anesthetic State Transitions

UnCheol Lee, Ph.D.,* Markus Müller, Ph.D.,† Gyu-Jeong Noh, M.D., Ph.D.,‡ ByungMoon Choi, M.D.,§ George A. Mashour, M.D., Ph.D.‖

ABSTRACT

Background: It is still unknown whether anesthetic state transitions are continuous or binary. Mathematical graph theory is one method by which to assess whether brain networks change gradually or abruptly upon anesthetic induction and emergence.

Methods: Twenty healthy males were anesthetized with an induction dose of propofol, with continuous measurement of 21-channel electroencephalogram at baseline, during anesthesia, and during recovery. From these electroencephalographic data a "genuine network" was reconstructed based on the surrogate data method. The effects of topologic structure and connection strength on information transfer through the network were measured independently across different states.

Results: Loss of consciousness was consistently associated with a disruption of network topology. However, recovery of consciousness was associated with complex patterns of altered connection strength after the initial topologic structure had slowly recovered. In one group of subjects, there was a precipitous increase of connection strength that was associated with reduced variability of emergence time. Analysis of regional effects on brain networks demonstrated that the parietal network was significantly disrupted, whereas the frontal network was minimally affected.

Conclusions: By dissociating the effects of network structure and connection strength, both continuous and discrete elements of anesthetic state transitions were identified. The study also supports a critical role of parietal networks as a target of general anesthetics.

What We Already Know about This Topic

- General anesthesia is characterized by a disruption of network communication, but whether this occurs in a continuous or stepwise fashion is unknown.

What This Article Tells Us That Is New

- Electroencephalographic data during induction of and emergence from propofol anesthesia in humans can be analyzed using graph theory to model network behavior.
- Both continuous and discrete elements were observed in transitions between the awake and anesthetized states, particularly in the parietal cortex.

CONTROVERSY persists as to whether anesthetic state transitions occur continuously, *via* "flip-flop" mechanisms, or by shifting phases. Theories of general anesthesia related to neural information synthesis would predict a graded, continuous transition from general anesthesia to consciousness during emergence.[1] Theories of general anesthesia that relate to sleep-wake neurobiology might predict a binary "flip-flop" from unconsciousness to consciousness.[2] Still other frameworks suggest that emergence relates to a number of discrete phase transitions.[3–5] It is also possible that anesthetic state transitions have both continuous and discrete components that can be dissociated. Furthermore, recent data suggest that anesthetic induction and emergence are not simply "mirror images" of one another, but are characterized by a distinct neurobiology.[2,6] The nature of anes-

* Postdoctoral Research Fellow, Department of Anesthesiology, University of Michigan Medical School, Ann Arbor, Michigan. † Associate Professor, Facultad de Ciencias, Universidad Autónoma del Estado de Morelos, Cuernavaca, México. ‡ Professor and Chair, Department of Clinical Pharmacology and Therapeutics, Department of Anesthesiology and Pain Medicine, Asan Medical Center, University of Ulsan College of Medicine, Seoul, Korea. § Public Health Physician, Department of Anesthesiology and Pain Medicine, National Medical Center, Seoul, Korea. ‖ Assistant Professor of Anesthesiology and Neurosurgery, Director of Neuroanesthesiology, Faculty, Neuroscience Graduate Program, University of Michigan Medical School.

Received from the University of Michigan Medical School, Ann Arbor, Michigan. Submitted for publication September 1, 2010. Accepted for publication December 22, 2010. Supported by departmental funds, as well as the National Institutes of Health, Bethesda, Maryland, KL2 RR024987-01 (to Dr. Mashour).

Address correspondence to Dr. Mashour: University of Michigan Medical School, 1H247 UH/SPC-5048, 1500 East Medical Center Drive, Ann Arbor, Michigan 48109-5048. gmashour@umich.edu. Anesthesiology 2011; 114: 872–81

MA Presented at the Best Abstracts of the Meeting Session of the American Society of Anesthesiologists Annual Meeting, October 18, 2010.

◆ This article is accompanied by an Editorial View. Please see: Pryor KO, Sleigh JW: The seven bridges of Königsberg. ANESTHESIOLOGY 2011; 114:739–40.

Supplemental digital content is available for this article. Direct URL citations appear in the printed text and are available in both the HTML and PDF versions of this article. Links to the digital files are provided in the HTML text of this article on the Journal's Web site (www.anesthesiology.org).

thetic induction and emergence will be important to clarify for a more precise understanding of general anesthetic mechanisms as well as for the development of more sophisticated intraoperative neurophysiologic monitors.

Analysis of network-level properties may be particularly suited to investigating anesthetic state transitions, because general anesthesia is characterized by a disruption of network communication.[7–17] Graph theory is one method by which to represent networks in the brain, where neural regions can be considered the *nodes* of the graph and the relationship between them the *edges*. Brain networks have a conserved organization across species and spatial scales that enable optimal information processing among distributed neural network elements.[18] This "small world" network organization is similar to that of an airport system, in which certain hubs act as densely connected nodes that can enhance the efficiency of travel. That two nodes are connected by an edge reflects the structure or *topology* of a network; however, edges may vary as reflected by their *connection strength*. Thus, global network efficiency in the brain can be deconstructed into the elements of topologic structure and connection strength (discussed further in the Materials and Methods section). By delineating the effects of general anesthesia on these two elements independently, we can more precisely characterize the network properties of anesthetic state transitions.

Using electroencephalographic data from human subjects, we tested the hypothesis that network topology and connection strength changed independently during anesthetic state transitions and that these changes could therefore be both discrete and continuous. Because of the significant increase of electroencephalographic power in lower-frequency bandwidths during general anesthesia, the correlation across nodes could be spurious. Thus, to achieve the objective of our study, we refined techniques to eliminate spurious network connections such that only "genuine" networks would be reconstructed and analyzed.[19,20] Finally, given the proposed importance of the frontal-parietal network in the mechanism of general anesthesia,[21–23] we assessed whether the components of network topology and connection strength were differentially altered in these brain regions.

Materials and Methods

Drug Administration and Electroencephalography

After institutional review board approval (Asan Medical Center, Seoul, Korea) and informed consent, 20 healthy human participants were studied with 21-channel electroencephalography. Three states were investigated: (1) baseline consciousness (eyes closed); (2) general anesthesia, defined as loss of response to the command "open your eyes" after induction with 2 mg/kg of the intravenous agent propofol (Diprivan®, AstraZeneca, London, United Kingdom); and (3) recovery from general anesthesia, defined by a return of responsiveness to the command "open your eyes." Electroencephalographic data on 10 of these subjects were originally gathered for a study of the frontoparietal system,[12] but underwent a completely different analysis for the current study; novel data from another 10 subjects were included for the current investigation. Each volunteer fasted for 8 h before study drug administration. We excluded volunteers who had known allergy to propofol, medical conditions, abnormal laboratory findings with clinical significance, or a body weight that was not within 30% of ideal range. The average age was 23 ± 2 yr (range, 20–28 yr).

An 18-gauge angiocatheter was placed in a vein of the antecubital area. Subjects received an initial intravenous bolus of 2.0 mg/kg of propofol. Time to loss of consciousness (LOC) was determined every 5 s by the loss of response to verbal command. If respiratory depression occurred, lungs were manually ventilated with 100% oxygen *via* facemask to maintain an end-tidal carbon dioxide concentration of 35–45 mmHg. Manual ventilation was discontinued when the spontaneous respiratory rate exceeded 12 breaths/min and end-tidal carbon dioxide was less than 45 mmHg. Time to return of consciousness (ROC) after the intravenous bolus of 2.0 mg/kg of propofol was determined by the recovery of response to verbal command; this assessment started 10 min after LOC. Upon completion of the measurement of electroencephalographic activity, subjects were transferred to the postanesthesia care unit, breathing room air. During the recovery period, subjects were monitored with electrocardiography, pulse oximetry, and noninvasive blood pressure measurement for 1 h. If vital signs were stable and full recovery from sedation was confirmed, the subject was discharged from the hospital.

The electroencephalograms of 21 channels (Fp1, Fp2, F3, F4, F5, F6, F7, F8, Fz, C3, C4, Cz, T7, T8, P3, P4, P5, P6, P7, P8, Pz referenced by A2, 10–20 system) were recorded with the subjects' eyes closed, with a sampling frequency of 256 Hz and 16-bit analog-to-digital precision by WEEG-32® (LXE3232-RF, Laxtha Inc., Daejeon, Korea). Baseline electroencephalography was recorded for 5 min before an intravenous bolus of propofol was administered. Electroencephalography was recorded continuously during and after the intravenous bolus of propofol and up to 10 min after ROC. Before the analysis of electroencephalographic data, a Fourier-based band-pass filter was applied to a frequency range of 0.5–55 Hz. Epochs with artifacts were eliminated from the analysis.

Reconstruction of "Genuine Networks" from Electroencephalographic Data

General anesthesia is associated with a marked increase in the power spectrum of lower-frequency waveforms.[24] In a finite-size dataset, lower-frequency power spectra of the electroencephalogram produce larger spurious cross-correlations. Müller *et al.* suggested a method to estimate genuine, spurious, and total cross-correlation strengths of multichannel electroencephalograms based on surrogate (*i.e.*, randomized)

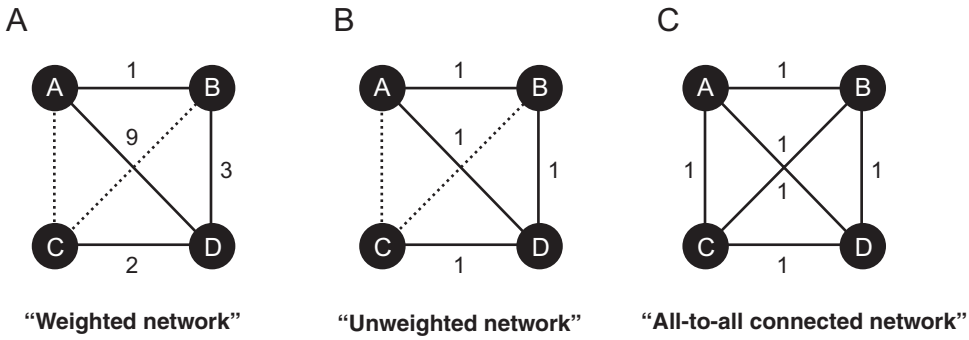

Fig. 1. Different types of networks that consist of four nodes. (*A*) Weighted network: a network weighted on edges by genuine correlation strengths; (*B*) unweighted network: a network that consists of only a connected (1) or unconnected state (0), without weighted values; (*C*) all-to-all connected network: a network in which all nodes are connected to one another. The connected nodes are denoted with a solid line, whereas the disconnected nodes are denoted with a dotted line.

electroencephalographic data.[20] For a given electroencephalographic dataset, spurious correlation strength c_s is estimated by the cross-correlation values of randomized data. The surrogate dataset has the same power spectra and the same data length as the original electroencephalographic data, but no genuine cross-correlation because of phase randomization.[25] Thus, if the surrogate data have a cross-correlation value, it must have resulted from the finite-size effect by a combination of the finite data length used and the power spectra of the given electroencephalogram. Genuine correlation strength of the original electroencephalographic data c_g is defined as the deviation from this randomized dataset. Both correlation strengths c_g and c_s are normalized values within 0 and 1.

Brain networks were constructed by using only genuine correlation strengths with 21-channel electroencephalography, which eliminates the analysis of spurious correlation effects during assessment of network properties. First, we calculated the genuine correlation strengths for all pairs of electroencephalogram channels, which were defined as the significant deviation from 1,000 pairs of randomized surrogate data for each pair of channels. If a pair of electroencephalogram channels had a nonzero genuine correlation, it was deemed to be connected. Conversely, if the nonzero correlation was not significantly deviated from the spurious correlation of the surrogate date set, the pair was deemed to be unconnected.

Global Efficiency of Genuine Networks

The anatomic and functional networks of the normal brain have a typical structure called "small world" organization, which is an optimal network structure for economic wiring and fast information transmission.[18,26] The hubs of the airport system also result in a small world network. This optimal network structure is slightly changed in various cognitive tasks, but significant disruptions have been reported in disease states such as epilepsy, schizophrenia, and dementia.[27–30] To quantify the overall state of a brain network with one index, we used a measure of global efficiency E_g. Global efficiency is a representative index for network properties and quantifies the information transmission capacity of a network.[18] By definition, if the correlation across nodes increases, the global efficiency also increases. However, global efficiency depends on both the topologic structure and correlation or connection strength of the nodes. For example, if the topologic structure is not amenable to efficient information transfer (as in a regular lattice structure), the increase in global efficiency would be small even though the correlation across nodes was large. Therefore, the decomposition of the effects of the two network elements (topologic structure and connection strength) on the global efficiency provides more detailed information about the network. In terms of neurophysiology, rapid changes in connection strength may be mediated by variations of synchronization.[31]

Consider graph G as an abstract representation of a network. It consists of a set of nodes (or vertices) and a set of edges (or connections). In a graph, we can find the shortest path between a certain pair of nodes. In figure 1A, for example, the shortest path between two nodes, "A" and "C," is A→B→D→C and the shortest path length is 6 (1 + 3 + 2). The path, A→B→D→C, is shorter than another path, A→D→C, based on the total weight of the path. Therefore, the shorter the mean path length over all pairs of nodes, the more efficient the information transmission is in a network. The global efficiency E_g quantifies the efficiency of information transmission of a network based on the average weight of edges that must be traversed to go from one node to another. By definition, the global efficiency E_g is the inverse of the average shortest path length ($1/d_{ij}$) over all pairs of nodes in a network G. It is defined as follows,

$$E_g = \frac{1}{N(N-1)} \sum_{i,j \in G,\, i \neq j} \frac{1}{d_{ij}}, \quad d_{ij} = \frac{1}{c_g(i,j)} \qquad (1)$$

where d_{ij} is the shortest path length between node i and j. The d_{ij} is defined with inverse genuine correlation strength $c_g(i, j)$. If $c_g(i, j) = 1$ for a perfectly coherent case, then $d_{ij} = 1$. On the other hand, if $c_g(i, j) = 0$ for a completely uncorrelated case, then d_{ij} is infinite. Therefore, the path length d_{ij} has a value between 1 and infinity. Here, the path length is defined

by the correlation between two neural events as a measure of functional similarity. It is important to stress that the "length" of the path has a *functional* definition rather than a spatial one. More strongly connected nodes are functionally "closer" to one another and therefore transfer information more efficiently. Consider the analogy of a cell phone and assume you had to transmit information to both a friend next door and a friend across town. If you were unable to call your friend next door because of lost connection strength, but were nonetheless able to call your friend across town, then you would have a functionally shorter path length to your cross-town friend in comparison with your spatially close neighbor.

However, the shortest path for a pair of nodes changes depending on the type of network. In a weighted network (fig. 1A), for instance, the shortest path between the node "A" and "C" is A→B→D→C with a path length of 6, instead of A→D→C with a path length of 11. The path length is different in the unweighted network (fig. 1B), even though it has the same connection structure. For the unweighted network, the shortest path length between the node "A" and "C" is A→D→C with a path length of 2, instead of A→B→D→C with a path length of 3. In the same connection structure, the connection strengths change the shortest path between nodes, implying that the arrangement of connection strengths in the network affects the information transmission capacity. It is also clear that the topologic structure affects the global efficiency. Therefore, the information transmission capacity of the network depends on the separate properties of network structure and connection strength. The all-to-all connected network is the ideal network in terms of information transmission (fig. 1C).

Dissociating the Effects of Network Structure and Connection Strength on Global Efficiency

We dissociated the effect of network structure and the effect of connection strength on information transmission in the anesthetized brain.

The contribution of connection strength to global efficiency e_{str} was defined as the ratio between the global efficiencies of a genuine network and an unweighted network (which has no contribution from strength because it is unweighted).

$$e_{str} = \frac{E_g}{E_b}$$

The unweighted network, in which all weights of genuine network connections less than or equal to 1 were replaced with 1, was constructed and the global efficiency was calculated as follows.

$$E_b = \frac{1}{N(N-1)} \sum_{i,j \in G,\, i \neq j} \frac{1}{d_{ij}^b}$$

where d_{ij}^b is the shortest path length between node i and j in the unweighted network.

The contribution of network structure to global efficiency e_{top} was defined as the ratio between the global efficiencies of the unweighted network and a totally connected network, in which all shortest path lengths are 1.

$$e_{top} = \frac{E_b}{E_t}$$

Because the global efficiency of the totally connected network is optimal under a given condition, the difference between global efficiencies for two networks results from only the specific structure of an unweighted network in the same connection strengths of edges. E_t is always 1 so it was used only for conceptual symmetry in both definitions. Both indices, e_{str} and e_{top}, have a value between 0 and 1.

Moving Window Method

We assumed that 12-s intervals of electroencephalographic data can maintain a stationary state. The electroencephalographic data were segmented with a 12-s electroencephalogram window moving at 4 s; for each window, the genuine, spurious, total correlation strengths, as well as the e_{str}, e_{top}, and E_g were calculated (see Supplemental Digital Content 1, which describes more detailed methods, http://links.lww.com/ALN/A679).

Pharmacokinetic Simulation

Based on the population pharmacokinetic and pharmacodynamic models of lipid emulsion propofol derived in a previous study,[32] stochastic and deterministic simulations for plasma and effect-site concentrations of propofol were performed using NONMEM 712 (ICON Development Solutions, Dublin, Ireland). The blood-brain equilibration rate constant (k_{e0}) of propofol in these models was obtained using the Bispectral Index as a surrogate measure of propofol effect on the central nervous system. Individual pharmacokinetic parameters included in simulations of propofol effect-site concentrations were calculated using the patient's age and point estimates of fixed effect parameters. Point estimates of fixed and random effect parameters were used in stochastic simulations. Variances of random effect (interindividual and residual) parameters were fixed at 0 in a deterministic simulation, which produces the same plasma and effect-site concentrations of propofol as predicted by a target-controlled infusion system. Two thousand stochastic simulations were conducted.

Statistical Analysis

For statistical analysis, the three states were separated into a total of six substates. The *B*aseline state was separated into B1 (from 0 to 2.5 min) and B2 (from 2.5 min to 5 min), the *A*nesthetized state was separated into A1 (0 to 2 min after LOC) and A2 (−2.5 to 0 min before ROC), and the *R*ecovery state was separated into R1 (0 to 2.5 min after ROC) and R2 (2.5 to 5 min after ROC). Because the duration of the anesthetized state is different for each subject, we separated

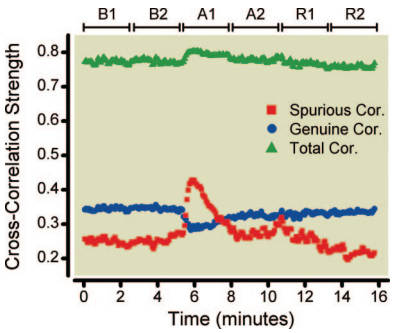

Fig. 2. The genuine and spurious correlation strengths across consciousness, anesthesia, and recovery. The average genuine, spurious, and total correlation strengths are displayed. The spurious correlation strength was significantly increased and the genuine correlation strength significantly decreased after loss of consciousness (around 5 min). The total correlation strength varied with the pattern of spurious correlation strength.

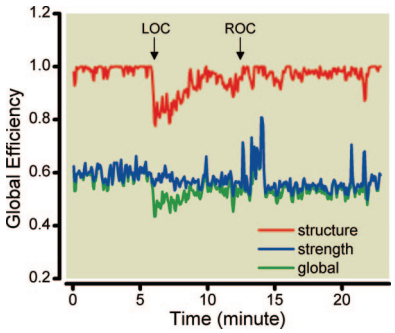

Fig. 3. Dissociation of two network effects on the global efficiency in a single subject. The effect of topologic structure and the effect of connection strength on the global efficiency are presented with the conventional global efficiency. It is apparent that the global efficiency pattern can be deconstructed to the topological structure and connection strength effects.

the substates based on the LOC and ROC times to facilitate statistical comparison. The correlation strengths, e_{str}, e_{top}, and E_g, were compared across the six substates; the significance was assessed by a repeated measures one-way ANOVA and a *post hoc* analysis using the Tukey multicomparison test. For the comparison of e_{str} and e_{top} between the frontal and parietal regions across six substates, the repeated measure two-way ANOVA and the *post hoc* analysis using the Bonferroni multicomparison test were applied. A P value of <0.05 was considered significant. The mean ± SD and the results of the *post hoc* test are presented in Supplemental Digital Contents 2–6 (http://links.lww.com/ALN/A680, http://links.lww.com/ALN/A681, http://links.lww.com/ALN/A682, http://links.lww.com/ALN/A683, http://links.lww.com/ALN/A684). The D'Agostino-Pearson omnibus normality test was conducted before performing the ANOVA test. A formal statistical consultation was obtained at the Center for Statistical Consultation and Research at the University of Michigan (Ann Arbor, MI), and the GraphPad Prism Version 5.01 (GraphPad Software Inc., San Diego, CA) was used.

Results

Spurious and Genuine Network Connections

The genuine, spurious, and total correlation strengths were altered after loss and recovery of consciousness during general anesthesia. Figure 2 presents the means of three correlation strengths in different states of consciousness. The spurious correlation strength significantly changed across the six substates ($F(5,95) = 19.2$, $P < 0.0001$), increasing after loss of consciousness and returning to the baseline level after the recovery state. By contrast, the genuine correlation strength showed the opposite change over the course of the experiment ($F(5,95) = 20.1$, $P < 0.0001$). The genuine correlation strength decreased after LOC and recovered quickly to the baseline level. The total correlation strength also significantly changed across states ($F(5,95) = 6.16$, $P < 0.0001$), increasing after LOC and returning to the original level by A2. Therefore, total correlation strength followed the spurious correlation strength pattern rather than the genuine correlation strength pattern in the anesthetized state (see Supplemental Digital Content 2, which is a table showing mean ± SD, http://links.lww.com/ALN/A680).

Dissociable Effects of Network Structure and Connection Strength

Figure 3 demonstrates the distinctive contributions of topology and connection strength to global efficiency in a single subject. The global efficiency of genuine network E_g is displayed together with the effects of network structure e_{top} and connection strength e_{str}, demonstrating distinct patterns of e_{str} and e_{top} at LOC and ROC. After LOC, e_{top} decreased steeply, whereas e_{str} decreased slowly; at ROC, e_{str} increased precipitously after e_{top} had already been restored. Data from this subject demonstrate that the temporal evolution patterns of e_{top} and e_{str} can be dissociable from one another and behave independently at LOC and ROC.

The individual and mean values of e_{top} and e_{str} for the 20 subjects are shown in figure 4. Based on the typical pattern of e_{str}, the subjects were classified according to two types of anesthetic responses. A subject was classified as "type 1" if there was a large increase of e_{str} at the ROC moment that exceeded the maximum e_{str} of the baseline state. If there was no increase of e_{str}, the subject was classified as "type 2." Eight of 20 subjects were classified as type 1 and the remaining 12 subjects were classified as type 2. Figure 3 is a salient example from the type 1 group. Figure 4A and 4B demonstrate the individual traces of e_{top} (upper tracing in each panel) and e_{str} (lower tracing in each panel) for type 1 and type 2 subjects; figure 4C and 4D demonstrate the average patterns of e_{top}, e_{str}, and E_g for type 1 and type 2 groups.

For both types, most values for e_{top} (topology) in the baseline state are close to 1, indicating that the brain network in this state has optimal information transmission capacity. The e_{top} of the type 1 group was significantly changed across

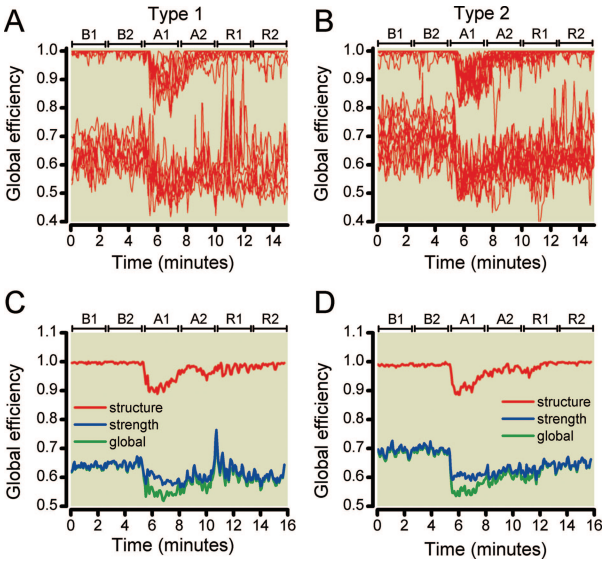

Fig. 4. Two types of anesthetic responses in brain networks. The subjects were classified into two types of groups based on the alterations of connection strength. (*A* and *B*) Individual traces of e_{top} (top tracing) and e_{str} (bottom tracing) for the type 1 (n = 8) and type 2 (n = 12) responses. (*C*) The mean values of the type 1 group in which the e_{str} showed a pattern of "slow decay and sudden return" at loss of consciousness (LOC) and recovery of consciousness (ROC). (*D*) By contrast, in the average trace of the type 2 group the e_{str} showed a pattern of "sudden decay and slow return" at LOC and ROC. Network topology e_{top} demonstrated a consistent response in all subjects.

the six substates ($F(5,35) = 10.5$, $P < 0.0001$). After induction with propofol, the e_{top} immediately decayed from 1 and gradually returned to the baseline level a few minutes *before* ROC. The e_{str} of the type 1 group also significantly changed across the six substates ($F(5,35) = 6.94$, $P < 0.0001$). After induction, it gradually decreased and recovered in the A2 state before ROC. After ROC, it was fully recovered to baseline level. The recovery process of e_{top} and e_{str} for the type 1 group began from the A2 state in the unconscious state.

For the type 2 response in figure 4D, both e_{top} and e_{str} significantly changed across the six substates ($F(5,55) = 17.07$, $P < 0.0001$; $F(5, 66) = 21.84$, $P < 0.0001$, respectively). The e_{top} decreased after LOC and recovered before ROC. The e_{str} also decreased after induction but was not fully recovered at the A2 period as was e_{top}, which already had a value comparable to those of the recovery states. The level of the baseline state recovered by the end of the experiment. This implies that the e_{str} was not fully recovered immediately after emergence but slowly returned to the original level. As a consequence, the behaviors of e_{str} in the A2 period (the period before emergence) and the R1 period (the period after emergence) were different between the type 1 and 2 groups.

During general anesthesia, e_{top} showed a similar anesthetic response pattern for most subjects, whereas e_{str} had two distinctive anesthetic response patterns. At induction and emergence, the e_{str} of the type 1 group showed a pattern of slow decay and sudden return; by contrast, the e_{str} of the type 2 group showed a pattern of sudden decay and slow return. Patterns of connection strength did not mirror changes in electroencephalographic power or high-frequency activity, suggesting that the observed changes were not due to electromyographic or other artifact (data not shown). (See Supplemental Digital Content 3–4 for tables including mean ± SD and statistical results, http://links.lww.com/ALN/A681, http://links.lww.com/ALN/A682.)

Table 1. Volunteer Characteristics

	Type 1 Emergence (n = 8)	Type 2 Emergence (n = 12)
Dose of propofol (mg)	151.9 ± 23.9	155.3 ± 26.2
Age (yr)	22.5 ± 1.4	23.7 ± 2.0
Weight (kg)	75.9 ± 12.0	77.6 ± 13.1
Height (cm)	177.5 ± 5.0	176.9 ± 5.3
LBM (kg)	59.7 ± 6.3	60.3 ± 6.8
BSA (m^2)	1.93 ± 0.15	1.94 ± 0.17

The volunteer characteristics were not significantly distinguishable between the two types of emergence with $P > 0.05$ in the t test and Mann–Whitney rank sum test. Data are stated as mean ± SD in the t-test and medians (25%, 75%) in Mann–Whitney rank sum test.

BSA = body surface area; LBM = lean body mass.

Pharmacologic and Behavioral Data for Type 1 and Type 2 Response Groups

Subject characteristics such as dose of propofol, age, weight, height, lean body mass, and body surface area were not distinguishable for subjects in the two response groups (table 1). Simulations did not reveal any statistically significant differences in the plasma or effect-site concentrations between the two groups (fig. 5). The volunteer responses during the study period are presented in table 2. Although times to LOC and ROC and the duration of unconsciousness failed to demonstrate statistically significant differences between the two groups, time to ROC and the duration of unconsciousness were more variable in the type 2 subjects: SD (type 1 *vs.* type 2) = 1.32 *versus* 3.78 min and 1.31 *versus* 3.74 min, respectively. Unusually delayed ROC was observed in one volunteer in the type 2 group (table 2). However, the tendency remained unchanged even if this volunteer was excluded from the analysis: SD of time to ROC and duration of unconsciousness (type 1 *vs.* type 2) = 1.32 *versus* 1.75 min and 1.31 *versus* 1.70 min, respectively. The percentage of volunteers who demonstrated consistently quiet behavior during the period of unconsciousness was twice as high in the type 1 group compared with the type 2 group (table 2).

Differential Effects in the Frontal and Parietal Lobes

In order to investigate local network properties, the same parameters demonstrated in figure 4 were measured in the frontal network (with nine electroencephalogram channels) and the parietal network (with seven electroencephalogram

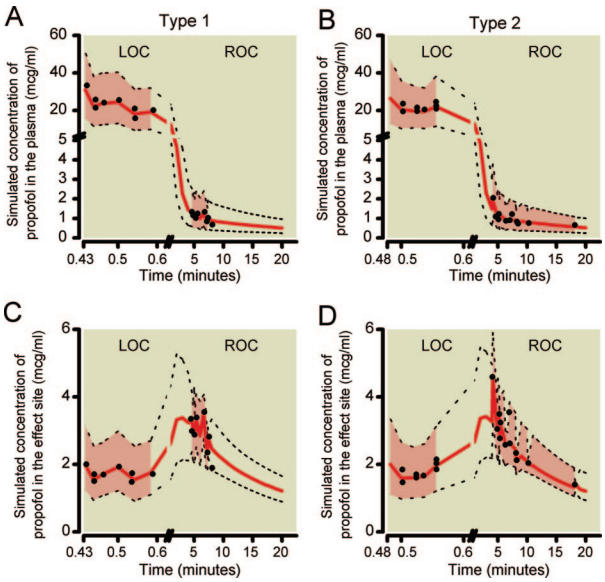

Fig. 5. Simulated concentrations of propofol in the plasma (*Cp*, *A* and *B*) and effect-site (*Ce*, *C* and *D*) after an intravenous bolus of propofol 2 mg/kg in volunteers showing type 1 (*A* and *C*) and 2 (*B* and *D*) emergence, respectively. No values of *Cp* and *Ce* at loss of consciousness (LOC) and recovery of consciousness (ROC) demonstrated statistically significant differences between the two types of emergence. Numeric data on the plots are stated as mean ± SD (*t* test) or median (25%, 75%) (Mann–Whitney rank sum test). Median values (*solid lines*) with 90% CI (*dotted lines*) of simulated *Cp* and *Ce* in 2,000 stochastic simulations are shown. Shaded areas within 90% CI represent the periods during which LOC and ROC were observed. A *black dot* represents *Cp* or *Ce* in an individual, which corresponds to the event of LOC or ROC. These values were obtained by deterministic simulations.

channels). Figure 6 shows the average patterns of e_{top} and e_{str} over 20 subjects for the frontal and parietal networks. For both parameters (e_{top} and e_{str}), the repeated measures two-way ANOVA test (two factors: the state and the local network) yielded a significant main effect of state ($F(5,190) = 18.20$, $P < 0.0001$ for e_{top}; $F(5,190) = 17.56$, $P < 0.0001$ for e_{str}), a nonsignificant effect of brain region ($F(1,190) = 4.066$, $P = 0.0509$ for e_{top}; $F(1,190) = 3.61$, $P = 0.065$ for e_{str}), and a significant interaction between state and brain region ($F(1,190) = 18.12$, $P < 0.0001$ for e_{top}; $F(1,190) = 2.477$, $P = 0.0335$ for e_{str}). The *post hoc* analysis using the Bonferroni multicomparison test revealed significant differences between the frontal and parietal networks at the A1 state for both parameters (e_{top} and e_{str}) ($t(19) = 8.486$, $P < 0.001$ for e_{top}; $t(19) = 3.281$, $P < 0.01$).

The e_{top} of the frontal network was not significantly changed over the course of the experiment, maintaining the optimal information transmission capacity ($F(5,95) = 0.439$, $P = 0.82$). By contrast, the e_{top} of the parietal network significantly lost its optimal information transmission capacity during the period after induction (A1). The decrease of e_{str} took place in both local networks ($F(5,95) = 24.93$, $P < 0.0001$ for the frontal network; $F(5, 95) = 43.23$, $P < 0.0001$ for the parietal network), but the parietal network was more significantly disrupted than the frontal network in terms of information transmission. (See Supplemental Digital Content 5–6 for tables including mean ± SD and statistical results, http://links.lww.com/ALN/A683, http://links.lww.com/ALN/A684).

Discussion

The results of this investigation point to several dissociable network properties that may guide future study of network-level anesthetic mechanisms as well as inform the development of more sophisticated intraoperative neurophysiologic monitors. First, we identified that there is a high degree of spurious electroencephalographic cross-correlation after induction with anesthesia that drives the aggregate value of correlations. Spurious correlations must therefore be taken into account when making electroencephalographic determinations of behavioral state under general anesthesia. Second, we identified dissociable properties contributing to the global efficiency of the network. Alterations of network structure (topology) appeared to have a consistent behavior across all subjects, whereas changes in connection strength demonstrated two distinct patterns. This implies that analysis of topologic structure may be more reliable in assessing anesthetic states or transitions and also has implications for mechanisms of variable emergence. Third, our analysis revealed differential network effects in the frontal and parietal regions, with the parietal area network undergoing more marked disruption of information transmission capacity. This implies that decreased information processing in the parietal lobe may be a mechanism of general anesthesia and that the frontal lobe may be less informative regarding anesthetic state transitions.

Genuine Versus *Spurious Networks*

When analyzing nonstationary physiologic data such as that associated with the electroencephalogram, it is necessary to account for the finite-size effect, which is a fundamental problem of signal processing.[33] With a finite dataset the linear cross-correlation measure can have a correlation value, even though the observed data are random. In particular, such spurious correlation becomes more exaggerated when the frequency spectra contained are lower.[20] In our data, the spurious correlation strength significantly increased after LOC and moved in the direction opposite that of the change of genuine correlation strength. This finding suggests that during reconstruction of brain networks with electroencephalograms of the anesthetized patient, the genuine correlation strength must be calculated rather than conventional cross-correlation, which is conceptually the same as the total correlation strength and which is prone to artifact from spurious correlations.

Distinct Network Properties and Emergence Patterns

By deconstructing global efficiency into the components of network structure (topology) and connection strength, we

Table 2. Volunteer Responses in the Type 1 and Type 2 Groups

Type of Emergence	Time to LOC (min)	Time to ROC (min)	Duration of Unconsciousness (min)	Behaviors during Unconsciousness
1	0.47	4.65	4.20	Quiet
1	0.43	6.67	6.10	Quiet
1	0.53	8.00	7.50	Quiet
1	0.50	5.37	4.92	Quiet
1	0.45	7.35	6.85	Quiet
1	0.53	4.82	4.35	Head lift just before ROC
1	0.45	7.30	6.87	Body movement and writhing
1	0.57	5.12	4.58	Body movement, attempt to rise
2	0.53	6.30	5.80	Quiet
2	0.52	6.72	6.20	Quiet
2	0.52	5.28	4.73	Quiet
2	0.48	7.00	6.45	Quiet
2	0.48	10.05	9.57	Quiet
2	0.50	18.20	17.68	Delayed recovery
2	0.52	8.07	7.53	Snoring
2	0.50	8.17	7.62	Head lift during unconsciousness
2	0.55	4.90	4.38	Hand movement just after the administration of propofol
2	0.55	5.22	4.73	Head movement at LOC
2	0.55	5.30	4.82	Phonating
2	0.48	4.17	4.12	Head movement

LOC = loss of consciousness; ROC = recovery of consciousness. Time to LOC: 0.49* (0.45, 0.53) and 0.52 (0.49, 0.54) min in type 1 and type 2 emergence, respectively. Time to ROC: 6.0* (5.0, 7.3) min and 6.5 (5.3, 8.1) min in type 1 and type 2 emergence, respectively. Duration of unconsciousness: 5.6* (4.4, 6.9) min and 6.0 (4.7, 7.6) min, respectively. $P > 0.05$ *vs.* Type 2 emergence for all (Mann–Whitney rank sum test), stated as median (25%, 75%).

were able to observe that there can be both continuous and discrete changes. In particular, the connection strength spiked precipitously just before ROC in one group of subjects, while demonstrating a sudden decay and gradual return to baseline in another. Thus, there may not be a single theoretic framework that explains all features of anesthetic state transitions. Type 1 responses were characterized by different network properties behaving independently at induction and emergence, with network structure continuously returning to baseline well before ROC, followed by a discrete increase in connection strength that appeared to be a "cognitive ignition" for emergence. This interpretation is supported by the fact that there was less variability in emergence time for the type 1 responses, which was not accounted for by pharmacokinetic modeling. Given the redundant cortical arousal systems found in the brainstem and diencephalon[34]—as well as clinical experience of heterogeneous recovery from anesthesia—it is not surprising that there may be distinct pathways to emergence. However, significantly more study is required before making a direct link between the underlying neurobiology of sleep-wake states and our findings at the network level.

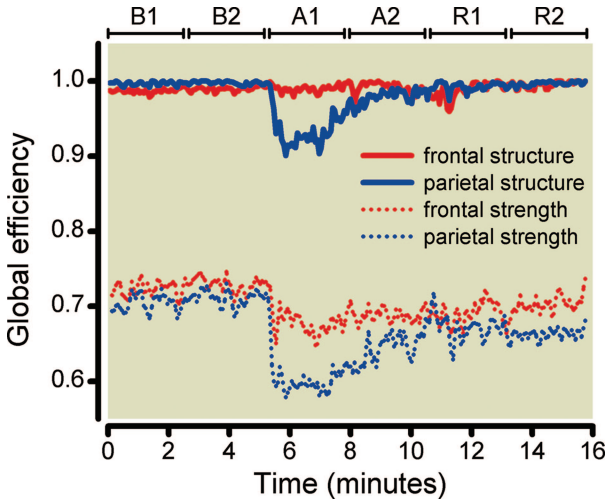

Fig. 6. The comparison of two network element effects in the frontal and parietal regions. The optimal topologic structure of the frontal network was maintained after loss of consciousness (in A1 state), while that of the parietal network was significantly disrupted. The decrease of connection strength was more pronounced for the parietal network compared to the frontal network.

Evidence for an Important Role of Parietal Processing

The inhibition of information processing in the frontoparietal system is thought to be a mechanism of general anesthesia, which is not surprising given the multiple roles of this system in consciousness, attention, and memory.[35] We and others have found that there is a selective inhibition of feedback activity from frontal to parietal regions in association with anesthetic-induced unconsciousness.[9,12] It is unclear, however, whether the frontal lobe plays a critical role in anesthetic hypnosis induced by different agents.[36] Hudetz[23] has suggested that an agent-invariant "final common pathway" to unconsciousness may be the disruption of informa-

tion integration in a network of the posterior parietal cortex. It is possible that the critical change in cortical information transfer within local circuits of the posterior parietal cortex leads to a generalized failure of information synthesis. Our data support Hudetz's hypothesis. Further supporting data for a critical role of the parietal region are derived from a computational modeling study. Computational "lesioning" based on anatomic connectivity data from the macaque monkey demonstrated that lesions of parietal regions had the greatest potential to disrupt the integrative aspects of neocortical function.[37] Our data regarding the differential effects of frontal and parietal networks have clinical relevance, because most cerebral function monitors developed for the detection of anesthetic state transitions are based on electrophysiologic recording from the frontal region.

Limitations

There are numerous limitations to our study. First, our subjects were young, healthy males and an induction dose of only one intravenous anesthetic was tested. Ongoing studies are examining state transitions with graded delivery of propofol and sevoflurane in a surgical population of both sexes. Second, data used in the current study were originally gathered for a study of anesthetic induction rather than both induction and emergence. Thus, the fact that there was not a steady-state change in anesthetic dosing implies that drug concentration in the brain was changing far more rapidly at induction than emergence, which limits interpretations of the neurobiologic differences between the two due to asymmetry. Third, 21-channel electroencephalography has suboptimal spatial resolution, so data regarding the role of frontal and parietal regions in anesthetic-induced hypnosis must be interpreted cautiously. Fourth, we are unable to explain why propofol was associated with two distinct responses of connection strengths (type 1 and type 2), but based on our modeling data the finding does not appear to relate to pharmacologic differences between the two response groups. These data should be regarded as hypothesis-generating.

Conclusion

By dissociating the effects of network structure and connection strength, we have identified both continuous and discrete elements of anesthetic state transitions using propofol. Furthermore, we have identified variations in emergence patterns that relate to network connection strength. Finally, our data support a critical role of parietal networks as a target of general anesthetics.

References

1. Alkire MT, Hudetz AG, Tononi G: Consciousness and anesthesia. Science 2008; 322:876–80
2. Kelz MB, Sun Y, Chen J, Cheng Meng Q, Moore JT, Veasey SC, Dixon S, Thornton M, Funato H, Yanagisawa M: An essential role for orexins in emergence from general anesthesia. Proc Natl Acad Sci USA 2008; 105:1309–14
3. Walling PT, Hicks KN: Nonlinear changes in brain dynamics during emergence from sevoflurane anesthesia: Preliminary exploration using new software. Anesthesiology 2006; 105: 927–35
4. Steyn-Ross ML, Steyn-Ross DA, Sleigh JW, Wilcocks LC: Toward a theory of the general-anesthetic-induced phase transition of the cerebral cortex. I. A thermodynamics analogy. Phys Rev E 2001; 64:011917
5. Steyn-Ross DA, Steyn-Ross ML, Wilcocks LC, Sleigh JW: Toward a theory of the general-anesthetic-induced phase transition of the cerebral cortex. II. Numerical simulations, spectral entropy, and correlation times. Phys Rev E 2001; 64:011918
6. Friedman EB, Sun Y, Moore JT, Hung HT, Meng QC, Perera P, Joiner WJ, Thomas SA, Eckenhoff RG, Sehgal A, Kelz MB: A Conserved behavioral state barrier impedes transitions between anesthetic-induced unconsciousness and wakefulness: Evidence for neural inertia. PLoS ONE 2010; 5:e11903
7. White NS, Alkire MT: Impaired thalamocortical connectivity in humans during general-anesthetic-induced unconsciousness. Neuroimage 2003; 19:402–11
8. Peltier SJ, Kerssens C, Hamann SB, Sebel PS, Byas-Smith M, Hu X: Functional connectivity changes with concentration of sevoflurane anesthesia. Neuroreport 2005; 16:285–8
9. Imas OA, Ropella KM, Ward BD, Wood JD, Hudetz AG: Volatile anesthetics disrupt frontal-posterior recurrent information transfer at gamma frequencies in rat. Neurosci Lett 2005; 387:145–50
10. Imas OA, Ropella KM, Wood JD, Hudetz AG: Isoflurane disrupts anterio-posterior phase synchronization of flash-induced field potentials in the rat. Neurosci Lett 2006; 402:216–21
11. Lee U, Mashour GA, Kim S, Noh GJ, Choi BM: Propofol induction reduces the capacity for neural information integration: Implications for the mechanism of consciousness and general anesthesia. Conscious Cogn 2009; 18:56–64
12. Lee U, Kim S, Noh GJ, Choi BM, Hwang E, Mashour GA: The directionality and functional organization of frontoparietal connectivity during consciousness and anesthesia in humans. Conscious Cogn 2009; 18:1069–78
13. Martuzzi R, Ramani R, Qiu M, Rajeevan N, Constable RT: Functional connectivity and alterations in baseline brain state in humans. Neuroimage 2010; 49:823–34
14. Ferrarelli F, Massimini M, Sarasso S, Casali A, Riedner BA, Angelini G, Tononi G, Pearce RA: Breakdown in cortical effective connectivity during midazolam-induced loss of consciousness. Proc Natl Acad Sci USA 2010; 107:2681–6
15. Mhuircheartaigh RN, Rosenorn-Lanng D, Wise R, Jbabdi S, Rogers R, Tracey I: Cortical and subcortical connectivity changes during decreasing levels of consciousness in humans: A functional magnetic resonance imaging study using propofol. J Neurosci 2010; 30:9095–102
16. Boveroux P, Vanhaudenhuyse A, Bruno MA, Noirhomme Q, Lauwick S, Luxen A, Degueldre C, Plenevaux A, Schnakers C, Phillips C, Brichant JF, Bonhomme V, Maquet P, Greicius MD, Laureys S, Boly M: Breakdown of within- and between-network resting state functional magnetic resonance imaging connectivity during propofol-induced loss of consciousness. Anesthesiology 2010; 113:1038–53
17. Lee U, Oh G, Kim S, Noh G, Choi B, Mashour GA: Brain networks maintain a scale-free organization across consciousness, anesthesia, and recovery: Evidence for adaptive reconfiguration. Anesthesiology 2010; 113:1081–91
18. Bullmore E, Sporns O: Complex brain networks: Graph theoretical analysis of structural and functional systems. Nat Rev Neurosci 2009; 10:186–98
19. Rummel C, Müller M, Baier G, Amor F, Schindler K: Analyzing spatio-temporal patterns of genuine cross-correlations. J Neurosci Methods 2010; 191:94–100
20. Müller M, Baier G, Rummel C, Schindler K: Estimating the strength of genuine and random correlations in non-stationary multivariate time series. Eur Phys Lett 2008; 84:10009

21. Alkire MT: Loss of effective connectivity during general anesthesia. Int Anesthesiol Clin 2008; 46:55–73
22. Hudetz AG: Suppressing consciousness: Mechanisms of general anesthesia. Semin Anesth 2006; 25:196–204
23. Hudetz AG: Cortical disintegration mechanism of anesthetic-induced unconsciousness, in Suppressing the Mind, 1st edition. Edited by Hudetz AG, Pearce R, Humana Press, 2010, pp 99–126
24. John ER, Prichep LS: The anesthetic cascade: A theory of how anesthesia suppresses consciousness. ANESTHESIOLOGY 2005; 102:447–71
25. Schreiber T, Schmitz A: Surrogate time series. Physica D 2000; 142:346–82
26. Sporns O, Tononi G, Kötter R: The human connectome: A structural description of the human brain. PLoS Comput Biol 2005; 1:e42
27. Micheloyannis S, Pachou E, Stam CJ, Breakspear M, Bitsios P, Vourkas M, Erimaki S, Zervakis M: Small-world networks and disturbed functional connectivity in schizophrenia. Schizophr Res 2006; 87:60–6
28. Liu Y, Liang M, Zhou Y, He Y, Hao Y, Song M, Yu C, Liu H, Liu Z, Jiang T: Disrupted small-world networks in schizophrenia. Brain 2008; 131:945–61
29. Ponten SC, Bartolomei F, Stam CJ: Small-world networks and epilepsy: Graph theoretical analysis of intracerebrally recorded mesial temporal lobe seizures. Clin Neurophysiol 2007; 118:918–27
30. Kramer MA, Kolaczyk ED, Kirsch HE: Emergent network topology at seizure onset in humans. Epilepsy Res 2008; 79:173–86
31. Stam CJ, Hillebrand A, Wang H, Mieghem PV: Emergence of modular structure in a large-scale brain network with interactions between dynamics and connectivity. Front Comput Neurosci 2010; 4:133
32. Kim KM, Choi BM, Park SW, Lee SH, Christensen LV, Zhou J, Yoo BH, Shin HW, Bae KS, Kern SE, Kang SH, Noh GJ: Pharmacokinetics and pharmacodynamics of propofol microemulsion and lipid emulsion after an intravenous bolus and variable rate infusion. ANESTHESIOLOGY 2007; 106:924–34
33. Kantz H, Schreiber T: Nonlinear time series analysis, 2nd Edition, Edited by Kantz H, Schreiber T, Cambridge University Press, 2004, pp 13–27
34. Franks NP: General anaesthesia: From molecular targets to neuronal pathways of sleep and arousal. Nat Rev Neurosci 2008; 9:370–86
35. Naghavi HR, Nyberg L: Common fronto-parietal activity in attention, memory, and consciousness: Shared demands on integration? Conscious Cogn 2005; 14:390–425
36. Veselis RA, Feshchenko VA, Reinsel RA, Dnistrian AM, Beattie B, Akhurst TJ: Thiopental and propofol affect different regions of the brain at similar pharmacologic effects. Anesth Analg 2004; 99:399–408
37. Honey CJ, Sporns O: Dynamical consequences of lesions in cortical networks. Hum Brain Mapp 2008; 29:802–9